Diagn Interv Radiol 2007; 13:56-60

Comparison of FSE T2W and 3D FIESTA sequences in the evaluation of posterior fossa cranial nerves with MR cisternography

Hatice Gül Hatipoğlu, Tuğba Durakoğlugil, Deniz Cılız, Enis Yüksel

PURPOSE
The aim of this study was to compare 3D fast imaging with steady state acquisition (3D FIESTA) to fast spin echo T2-weighted (FSE T2W) MRI sequences in the imaging of cisternal parts of cranial nerves V–XII.

MATERIALS AND METHODS
We retrospectively evaluated the temporal MRI sequences of 50 patients (F:M ratio, 27:23; mean age, 44.5 ± 15.9 years) who were admitted to our hospital with vertigo, tinnitus, and hearing loss. In all, we evaluated 800 nerves. Two radiologists, working independently, divided the imaging findings into 3 groups: 0 (not visualized), 1 (partially visualized), and 2 (completely visualized).

RESULTS
The rate of visualization of these cranial nerves with FSE T2W and 3D FIESTA sequences, respectively, (partially and completely visualized) were as follows: nerve V (100% and 100%); nerve VI (43% and 98%); nerve VII (100% and 100%); nerve VIII (100% and 100%); nerve IX–XI complex (67% and 100%); nerve XII (2% and 91%).

CONCLUSION
3D FIESTA sequences are superior to FSE T2W sequences in the imaging of cisternal parts of the posterior fossa nerves. 3D FIESTA sequences may be used for obtaining high-resolution MR cisternography images.

Key words: • *magnetic resonance imaging* • *cranial nerves* • *cisternography*

Prior to posterior fossa surgery, the connection between the tumoral lesion and neurovascular structures must be known. The importance of neuroradiological methods in the detection of inflammation and vascular pathologies affecting cranial nerves is widely known. Because magnetic resonance imaging (MRI) has high spatial and contrast resolution, cranial nerves are visible from their nuclei to their exiting levels at the cranium (1). New MRI sequences are capable of demonstrating the anatomy and pathology of cranial nerves (2). Neural structures and vessels in cerebrospinal fluid (CSF), and the connection with dura mater are seen with MR cisternography. The purpose of this study was to compare 3D fast imaging with steady state acquisition (3D FIESTA) to fast spin echo T2Weighted (FSE T2W) sequences in the imaging of cisternal parts of cranial nerves V–XII.

Materials and methods

Temporal MRI sequences of 50 patients (F:M ratio, 27:23; mean age, 44.5 ± 15.9 years) who were admitted with vertigo, tinnitus, and hearing loss were retrospectively evaluated. A 1.5 Tesla MR device (Excite, GE Medical systems, Milwaukee, Wisconsin, USA) was used in this study and gradient power was 33 mT/s. Axial T1W, T2W, 3D FIESTA, and post-contrast axial and coronal T1W sequences are used for routine temporal MRI in our department and gadolinium 0.2 ml/kg is used as contrast agent. Our parameters for imaging were as follows: T1W (TR, 500 ms; TE, 15.7 ms; slice thickness, 3 mm; interslice gap, 0.5 mm; FOV, 20 × 20 cm; matrix, 320 × 224; NEX, 3); T2W (TR, 3000 ms; TE, 104.8 ms; slice thickness, 3 mm; interslice gap, 0.5 mm; FOV, 20 × 20 cm; matrix, 320 × 224; NEX, 3); 3D FIESTA (TR, 4.8 ms; TE, 1.4 ms; slice thickness, 0.5 mm; FOV, 18 × 18 cm; matrix, 352 × 192; NEX, 4). T2W images were obtained with FSE sequences. Two radiologists, working independently, divided the imaging findings of the cisternal parts of cranial nerves V–XII into 3 groups: 0 (not visualized); 1 (partially visualized); 2 (completely visualized).

Evaluation with Kappa statistics revealed agreement between the observations of 2 researchers. In total, 800 nerves were evaluated. Cisternal parts of cranial nerves V–XII were visualized from their nuclei to their foraminal parts in all axial sequences. Statistical analyses were performed with the SPSS 11.5 software program (SPSS Inc., Chicago, Illinois, USA). Parametrical statistical methods were used for determining the visibility of cranial nerves in different MRI sequences.

Results

In all, 800 nerves in 50 patients were evaluated in our study. Trigeminal (Fig. 1), and facial and vestibulocochlear (Fig. 2) nerves were visualized with both FSE T2W and 3D FIESTA sequences. We did not visualize 57 of the abducens nerves (Fig. 3) with FSE T2W sequences nor

From the Department of Radiology (H.G.H. ✉ *gulhatip@yahoo.com*), Ankara Numune Research and Training Hospital, Ankara, Turkey.

Received 16 November 2006; revision requested 22 January 2007; revision received 4 February 2007; accepted 14 February 2007.

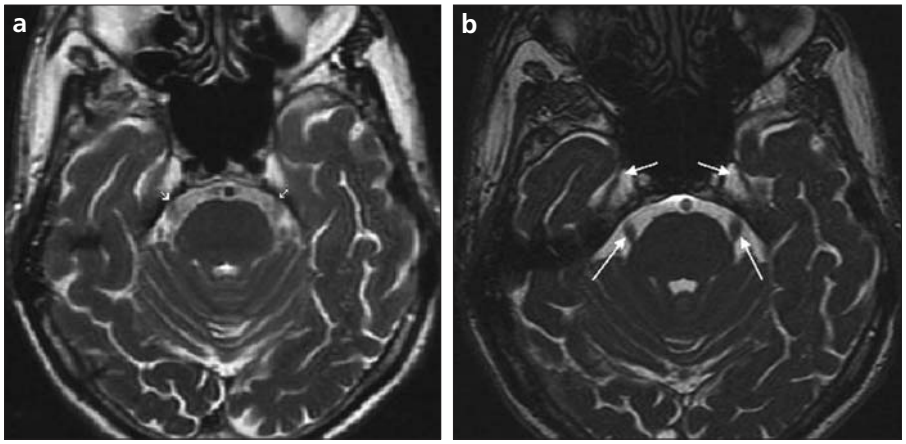

Figure 1. a, b. Cranial nerve V. On axial FSE T2W MR image **(a)** only the cisternal part of nerve V is visible *(arrows)*. On axial 3D FIESTA MR image **(b)**, cisternal part of nerve V *(long arrows)* and its branches in Meckel's cave are visible *(short arrows)*.

Success rates of 3D fast imaging with steady state acquisition (3D FIESTA) and fast spin echo T2-weighted (FSE T2W) MRI sequences in visualizing cranial nerves

		3D FIESTA		FSE T2W	
Nerve	Group[a]	Number of patients	%	Number of patients	%
V	2	100	100	100	100
	1	0	0	0	0
	0	0	0	0	0
VI	2	95	95	20	20
	1	3	3	23	23
	0	2	2	57	57
VII	2	100	100	100	100
	1	0	0	0	0
	0	0	0	0	0
VIII	2	100	100	100	100
	1	0	0	0	0
	0	0	0	0	0
IX–XI (lower nerve complex)	2	96	96	55	55
	1	4	4	12	12
	0	0	0	33	33
XII	2	64	64	1	1
	1	27	27	1	1
	0	9	9	98	98

[a] Group 0: not visualized; Group 1: partially visualized; Group 2: completely visualized

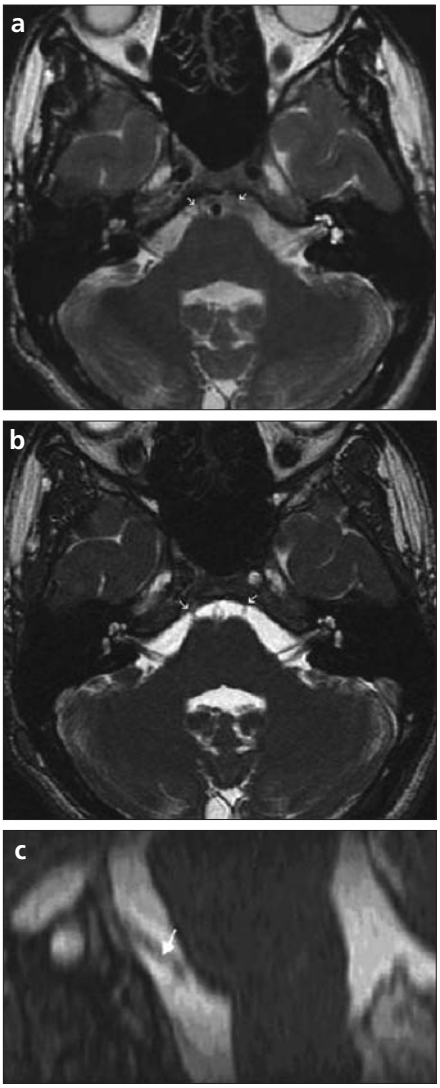

Figure 2. a–c. Cranial nerve VI. In axial FSE T2W MR image **(a)** nerve VI can be roughly visualized *(arrows)*. In axial 3D FIESTA MR image **(b)** and sagittal MIP reconstruction MR image **(c)**, it can be visualized clearly *(arrows in* **b** *and* **c***)*.

9 of them with 3D FIESTA sequences. Thirty-three of the lower cranial nerve complex (glossopharyngeal, vagus, and accessory nerves) nerves could not be visualized with FSE T2W, whereas, all of them were visualized with 3D FIESTA sequences (Fig. 4) . Ninety-eight and 9 of hypoglossal nerves were not visualized with FSE T2W and 3D FIESTA sequences, respectively (Fig. 5).

Visualization rates of all these cranial nerves (partially and completely visualized) with FSE T2W and 3D FIESTA sequences, respectively, were as follows: trigeminal nerve (100% and 100%); abducens nerve (43% and 98%); facial nerve (100% and 100%); vestibulocochlear nerve (100% and 100%); lower cranial nerve complex (glossopharyngeal, vagus, and accessory nerves) (67% and 100%); hypoglossal nerve (2% and 91%). Results are shown in Table.

Discussion

Visualizing the connection between tumoral lesions and neighboring neurovascular structures prior to posterior fossa surgery affects the success of the

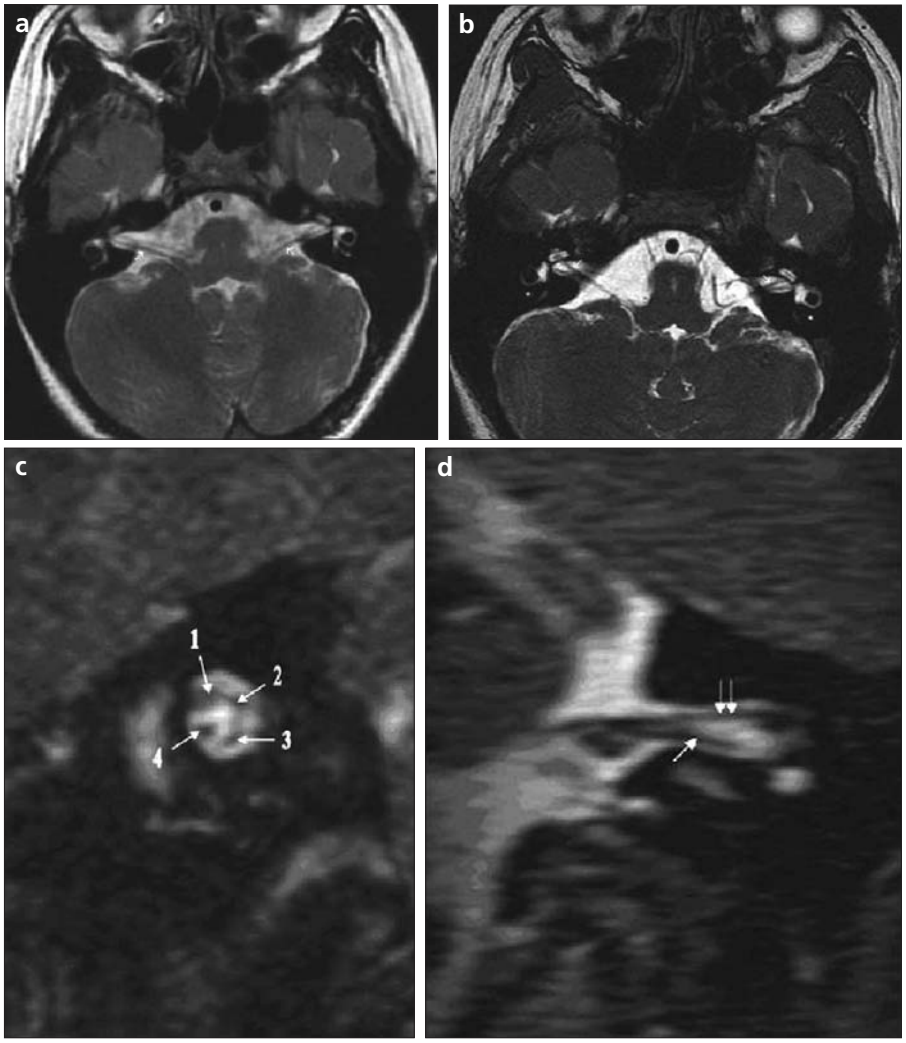

Figure 3. a–d. Cranial nerves VII and VIII. On axial FSE T2W MR image **(a)**, nerves VII and VIII can be roughly visualized *(arrows)*. On axial 3D FIESTA MR image **(b)** and coronal *(***c,** *arrow 1:* facial nerve; *arrow 2:* superior vestibular nerve; *arrow 3:* inferior vestibular nerve; *arrow 4:* cochlear nerve*)*, and sagittal *(***d,** *double arrows:* VII. nerve; *single arrow:* VIII. nerve*)* MIP reconstructions of 3D FIESTA sequences, all segments of the nerve complex are visible.

procedure. Invasive methods such as pneumoencephalography and high-resolution tomodensitometry have been performed in the past to show the cranial nerves using air and ionized contrast agents (3). Today, MRI is preferred because it is non-invasive, does not use radiation, has multiplanar imaging capability, and has new sequences showing structures <1 mm. Pre-contrast and post-contrast T1W and T2W sequences are frequently used in most radiology departments. These sequences can show cranial nerve nuclei, demyelination, inflammation, ischemic disorders, and vascular pathologies affecting the brain stem (4). Nonetheless, due to thick slices, calculation of tumoral volume with MRI is impossible. Borders of a tumoral lesion and its connection to nearby structures may be seen roughly. Cranial nerves have low signal intensity, unless they show contrast enhancement. Using contrast agents increases both the cost of imaging and may cause allergic reactions.

Recently, a connection between tumoral lesions, and small vessels and nerve branches has become more important with the development of microsurgery methods. In cases of hemifacial spasm, and trigeminal and glossopharyngeal neuralgia, nearby vascular structures must be evaluated (5). Therefore, new sequences and 3D imaging methods have been developed and among them is MR cisternography. With this imaging method, neural structures, vessels, and dura mater are seen as low signal intensity in CSF, which is observed as high signal intensity. MR cisternography is more effective than other se-

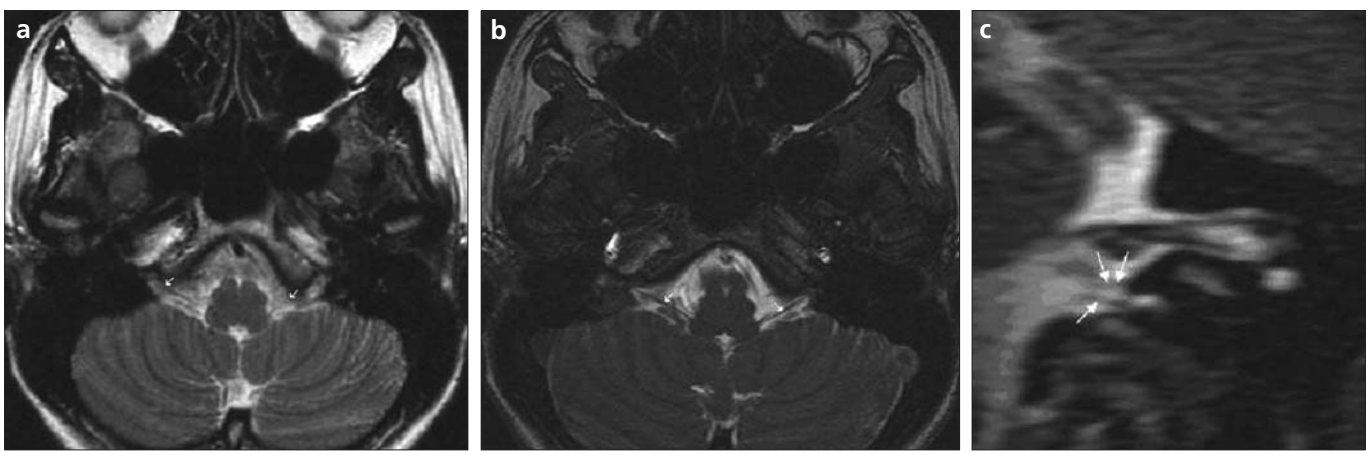

Figure 4. a–c. Cranial nerves IX–XI (lower nerve complex). On axial FSE T2W MR image **(a)** cranial nerves IX–XI cannot be clearly visualized *(arrows)*. On axial *(***b,** *arrows)* 3D FIESTA image MR and sagittal MIP reconstruction **(c)** of 3D FIESTA sequence, cisternal and foraminal parts of nerve IX *(double arrow in* **c***)* and nerve X *(single arrow in* **c***)* can be seen clearly. Nerve XI cannot be differentiated as a unique structure.

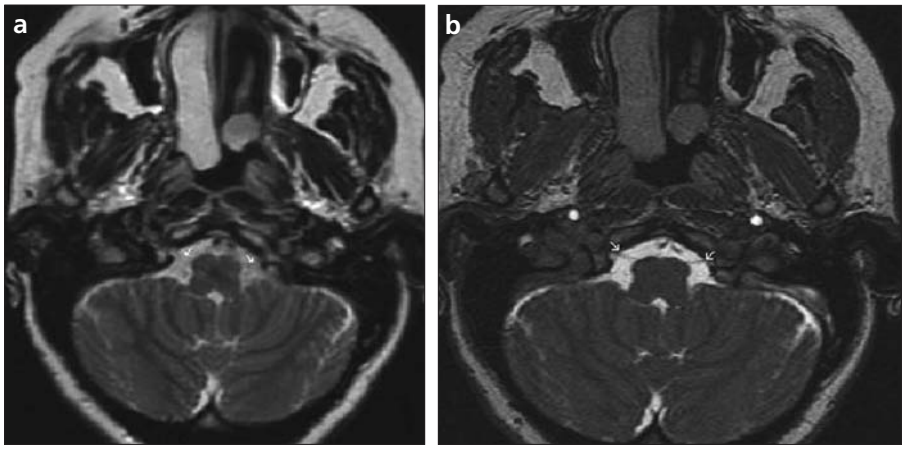

Figure 5. a, b. Cranial nerve XII. On axial FSE T2W MR image **(a)** cranial nerve XII cannot be evaluated. On axial 3D FIESTA MR image **(b)**, however, it can be clearly visualized *(arrows in* **a** *and* **b***)*.

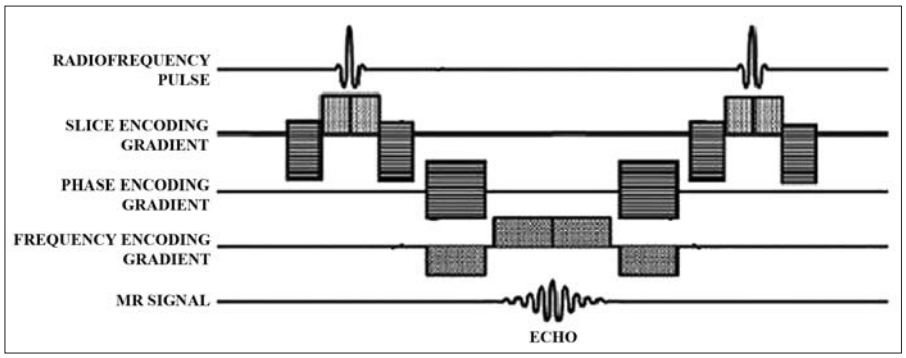

Figure 6. Pulse timing diagram of 3D FIESTA MRI sequence.

quences in evaluating anatomical structures of the subarachnoid space. It can be used for demonstrating the association between nearby structures and the posterior fossa or suprasellar tumoral lesions, and for differentiating intra-axial from extra-axial intracranial tumors.

MR cisternography can also be used for showing fistulas of the CSF in patients with rhinorrhea and for identifying the contours of aneurysms and their association with cranial nerves, dura mater, the cranial base, and brain parenchyma. It can be used for showing etiologies of a hemifacial spasm, and trigeminal and glossopharyngeal neuralgia. In the past, 3D fat suppressed T2W sequences were used for determining these images. Currently, sequences obtained with the steady state free precession (SSFP) method is preferred. These are gradient echo sequences and their relaxation time (TR) is shorter than tissue's T1 and T2 time. Radiofrequency (RF) pulses with a flip angle of <90° are sent to have short TR. In this situation, tissues always have longitudinal relaxation. Additionally, with the TRs used, transverse magnetization occurs. Transverse and longitudinal magnetization are never zero; they are in steady state. In this steady state, the transverse magnetization amplitude is higher in tissues that have a long T2 time. Among the repetition of RF pulses, the amount of transverse magnetization determines the amount of gained signal. In steady state sequences, the RF pulse repetition time is shorter than the tissue's transverse TR, so that T2 weighting is increased and T1 weighting is decreased. RF pulses are sent rapidly and repeatedly. Differing from spin echo sequences, in addition to signal echo, the sum of all signals that are composed by stimulated echo and free induction decay contribute to image formation, so that the signal is stronger. Stimulated echo occurs just after the third pulse, after the same time interval between the first 2 pulses. The power of the echo partially depends on T1 TR because excitation is stored as longitudinal magnetization between the second and third RF pulses. In SSFP sequences, all of the signals accumulate due to the balance of gradients in all three dimensions. Accordingly, images with a high signal to noise ratio are achieved. CSF, blood, and fat have long T2 and T1 TRs, so that they have high signal intensity. Imaging time is dependent on relaxation time. Gradient echo sequences that have short TRs occur in a shorter time than spin echo sequences. Images are obtained rapidly with SSFP sequences, so that they are preferred in cardiac and thoracoabdominal MR angiography.

Due to the fast imaging, movement and flow artifacts occur less often than with other sequences. The contrast to noise ratio (CNR) is higher, although it has a low contrast ratio (CR). Blurring artifacts occur less often because the MR signal is always achieved in a coherent state. Magnetic susceptibility artifacts occur with lower frequency due to very short TE and wide band thickness. The most frequently used SSFP sequences are bFFE, bTFE, true FISP, and FIESTA (6, 7). A pulse timing diagram of a 3D FIESTA sequence is shown in Fig. 6.

There are few studies in the literature about MR cisternography with 3D FIESTA sequences (5, 8, 9). Mikami et al. showed the volume of tumoral lesions, and their borders and connection with nearby structures in 23 cases (12 schwannomas, 8 meningiomas, and 3 epidermoid tumors) before surgery (8). Okumura et al. examined 66 nerves in 11 cases, visualizing all cranial nerves IX and X, and 91% of cranial nerves XI with MR cisternography and 3D FIESTA sequences (9). Chavez et al. showed the trigeminal nerve complex (nerve root entrance, trigeminal ganglion, nerve roots, and vascular structures) in 14 of 15 patients before radiotherapy. In one patient, the connection with vascular structures could not be clearly evaluated, but other characteristics were shown (5). In a study performed with another SSFP sequence, 3D bFFE, the CNR was high (10). Detailed images of the cerebellopontine angle with 3D bFFE, without CSF pulsation artifacts, were demonstrated in the same study because the bFFE sequence has a short TR and images are achieved faster.

Two true FISP sequences obtained with different RF pulses are combined to compose the 3D constructive interference of steady state (3D CISS) and high-resolution 3D T2W images are obtained (11). The 3D CISS sequence was first used by Casselman et al. for detailed evaluation of the inner ear and cerebellopontine angle (12). High-reso-

lution images are obtained by providing contrast between cranial nerves and CSF with CISS, heavy T2W spin echo, and 3D fast asymmetric spin echo (3D FASE) sequences (4, 13). However, in these sequences, the posterior fossa cranial nerves cannot be sufficiently visualized because of CSF artifacts at the level of the brain stem, which are due to the long TR of SSFP sequences and the long time images take to form (14). In a study comparing CISS and post-contrast T1W sequences, CISS was more successful in showing significant parameters, such as the connection between tumors and nearby tissues, which may affect the result of surgery (15). In another study, 2D post-contrast fat suppressed T1W (2D FS T1W) and 3D post-contrast magnetization-prepared rapid gradient echo (3D MP-RAGE) sequences were superior to FSE T2W sequences in the visualization of cranial nerves (16).

Driven equilibrium radiofrequency reset pulse (DRIVE) increases image quality and visualization of cranial nerves. If DRIVE turbo spin echo is performed after echo train, relaxation becomes fast and magnetization is balanced. When DRIVE is used, imaging time becomes short due to shortened TR and CSF flow artifacts decrease. High-resolution MR images can be obtained by adding DRIVE pulse to 3D spin echo T2W (3D TSE T2W) (14).

In this imaging study of cranial nerves, their entrance into the brain stem, cisternal parts, foraminal levels of hypoglossal, abducens, and lower cranial nerve complex were successfully demonstrated with 3D FIESTA sequences. As reported in other studies, T2W sequences were inadequate for such visualization (3, 4, 14). Cranial nerve XII exits from the medulla oblongata and extends to the hypoglossal canal. In the present study, 12% of hypoglossal nerves were visualized with FSE T2W, whereas 92% were with 3D FIESTA. FSE T2W failed to visualize 57% of abducens nerves, while 98% of them were visualized with 3D FIESTA. Therefore, 3D FIESTA sequences are preferred in determining disorders of cranial nerves VI–XII and the connection between these nerves and tumoral lesions. Cranial nerves IX–XI exit from their nuclei at the level of the medulla oblongata and extend to the foramen jugulare. These cranial nerves extend in close proximity to each other and are known as the lower cranial nerve complex, and 100% of lower cranial nerve complexes were visualized with 3D FIESTA, whereas 33% of them were not visualized with FSE T2W sequences. 3D FIESTA sequences are useful in the detection of glossopharyngeal neuralgia and may be useful prior to radiotherapy (5). The trigeminal nerve nucleus is located in the pons and nerve roots (ophthalmic, maxillary, and mandibular branches) extend to the prepontine cistern and enter into Meckel's cave. Trigeminal neuralgia may occur due to compression by small tortuous vessels at the level of prepontine cistern. Facial and vestibulocochlear nerve nuclei are located in the pons. These nerves enter the prepontine cistern and then extend into the internal acoustic canal. Facial and superior vestibular nerves are located superiorly, and cochlear and inferior vestibular nerves are located inferiorly in the internal acoustic canal. The trigeminal nerve, and facial and vestibulocochlear nerves may be visualized with FSE T2W sequences because they are thick; however, distinguishing ophthalmic, maxillary, and mandibular branches of the trigeminal nerve in Meckel's cave, and facial, superior, inferior vestibular, and cochlear nerves in the internal acoustic canal is possible with 3D FIESTA sequences. 3D FIESTA sequences may be used in patients scheduled for cochlear implant surgery (15). It is possible to successfully show the trigeminal nerve and connected nearby vascular structures, both before and after the surgery in trigeminal neuralgia cases (5). 3D FIESTA sequences can guide surgeons in calculating tumoral volume and in showing the connection between posterior fossa tumors and nearby structures (8). It accurately shows the entrance of the nerve and nearby vascular structures (5).

In conclusion, 3D FIESTA sequences are superior to FSE T2W sequences in visualizing cisternal parts of the posterior fossa cranial nerves for the following reasons: high-resolution, high quality images can be obtained; images are acquired in a short time; CSF pulsation and magnetic susceptibility artifacts decrease. Therefore, 3D FIESTA sequences can be used for obtaining MR cisternography images for visualization of the posterior fossa cranial nerves.

References

1. Pellicano G, Capaccioli L, Petacchi D, et al. Magnetic resonance in the study of the cranial nerves. Ital J Anat Embryol 1994; 99:229–241.
2. Laine FJ, Underhill T. Imaging of the lower cranial nerves. Magn Reson Imaging Clin N Am 2002; 10:433–449.
3. Seitz J, Held P, Strotzer M et al. MR imaging of cranial nerve lesions using six different high-resolution T1- and T2*-weighted 3D and 2D sequences. Acta Radiologica 2002; 43:349–353.
4. Yousry I, Camelio S, Schmid UD, et al. Visualization of cranial nerves I–XII: value of 3D CISS and T2-weighted FSE sequences. Eur Radiol 2000; 10:1061–1067.
5. Chavez GD, De Salles AA, Solberg TD, Pedroso A, Espinoza D, Villablanca P. Three-dimensional fast imaging employing steady-state acquisition magnetic resonance imaging for stereotactic radiosurgery of trigeminal neuralgia. Neurosurgery 2005; 56:628.
6. Konez O. Manyetik rezonans görüntüleme: temel bilgiler. İstanbul, Nobel. 1995; 53–78.
7. Huda W, Slone R. Review of radiological physics. Philadelphia, Lippincott Williams and Wilkins 1995; 171–193.
8. Mikami T, Minamida Y, Yamaki T, Koyanagi I, Nonaka T, Houkin K. Cranial nerve assessment in posterior fossa tumors with fast imaging employing steady-state acquisition (FIESTA). Neurosurg Rev 2005; 28:261–266.
9. Okumura Y, Suzuki M, Takemura A, et al. Visualization of the lower cranial nerves by 3D-FIESTA. Nippon Hoshasen Gijutsu Gakkai Zasshi 2005; 61:291–297.
10. Tsuchiya K, Aoki C, Hachiya J. Evaluation of MR cisternography of the cerebellopontine angle using a balanced fast-field-echo sequence: preliminary findings. Eur Radiol 2004; 14:239–242.
11. Yıldız S, Kaya A. Epidermoid tümörün görüntülenmesinde ve araknoid kistten ayırıcı tanısında CISS MRG sekansının rolü. Tani Girisim Radyol 2002; 8:3–9.
12. Casselman JW, Offeciers FE, Govaerts PJ, et al. Aplasia and hypoplasia of the vestibulocochlear nerve: diagnosis with MR imaging. Radiology 1997; 202:773–781.
13. Kakızawa Y, Hongo K, Takasawa H, et al. 'Real' three dimensional constructive interference in steady-state imaging to discern microneurosurgical anatomy. Technical note. J Neurosurg 2003; 98:625–630.
14. Ciftci E, Anik Y, Arslan A, Akansel G, Sarisoy T, Demirci A. Driven equilibrium (DRIVE) MR imaging of the cranial nerves V–VIII: comparison with the T2-weighted 3D TSE sequence. Eur J Radiol 2004; 51:234–240.
15. Kocaoglu M, Bulakbasi N, Ucoz T, et al. Comparison of contrast enhanced T1 weighted and 3D constructive interference in steady state images for predicting outcome after hearing-preservation surgery for vestibular schwannoma. Neuroradiology 2003; 45:476–481.
16. Seitz J, Held P, Frund R, et al. Visualization of the IXth to XIIth cranial nerves using 3-dimensional constructive interference in steady state, 3-dimensional magnetization-prepared rapid gradient echo and T2-weighted 2-dimensional turbo spin echo magnetic resonance imaging sequences. J Neuroimaging 2001; 11:160-164.